JOURNAL OF CATALYSIS 70, 418–432 (1981)

The Kinetics and Mechanism of Carbon Monoxide Hydrogenation over Alumina-Supported Ruthenium

C. STEPHEN KELLNER AND ALEXIS T. BELL

Materials and Molecular Research Division, Lawrence Berkeley Laboratory, and Department of Chemical Engineering, University of California, Berkeley, California 94720

Received January 29, 1981; revised April 2, 1981

A study was conducted of hydrocarbon synthesis from CO and H_2 over an alumina-supported Ru catalyst. Rate data for the formation of methane and C_2 through C_{10} olefins and paraffins were fitted by power law rate expressions. The kinetics observed experimentally can be interpreted in terms of a comprehensive mechanism for CO hydrogenation, in which CH_x (x = 0–3) species play a primary role. Expressions for the kinetics of methane synthesis, the kinetics and distribution of C_{2+} olefins and paraffins, and the probability of hydrocarbon chain growth derived from this mechanism are found to be in good agreement with the experimental results. The observed deviations from theory can be ascribed to secondary processes such as olefin hydrogenation and paraffin hydrogenolysis.

INTRODUCTION

During the past decade, extensive efforts have been made to understand the mechanism by which Group VIII metals catalyze the synthesize of hydrocarbons from CO and H_2 (*1–7*). One of the most important results of these investigations has been to draw attention to the importance of non-oxygenated surface intermediates. An increasing body of evidence now supports the hypothesis that hydrocarbon synthesis is initiated by the dissociation of CO and that the carbon atoms thus produced are hydrogenated to form adsorbed methylene and methyl groups. It has been proposed (*5–7*) that methyl groups act as precursors for the formation of methane as well as the growth of hydrocarbon chains, the latter process beginning with the insertion of a methylene group into the metal–carbon bond of a methyl group. Chain growth can continue by the further addition of methylene units to adsorbed alkyl species. Olefins and paraffins are finally produced from the alkyl moieties by either hydrogen elimination or addition.

A substantial part of the evidence supporting this view of hydrocarbon synthesis has been obtained from studies conducted with ruthenium catalysts. The emphasis on this metal can be explained by the fact that ruthenium produces, primarily, linear olefins and paraffins and relatively few oxygenated products. Moreover, unlike iron and cobalt, ruthenium is not converted to a carbide under reaction conditions. Studies by several authors (*8–11*) have shown that chemisorbed CO will dissociate on ruthenium at elevated temperatures to form adsorbed carbon atoms. Hydrogenation of this carbon occurs very readily to form methane as well as higher molecular weight paraffins. Ekerdt and Bell (*12*) have shown that carbon deposition also takes place during the steady-state reaction of CO and H_2, and that hydrogenation of this carbonaceous deposit following the elimination of chemisorbed CO produces a spectrum of hydrocarbon products. These latter results demonstrate that chain growth can occur in the absence of adsorbed CO. Further evidence for the participation of atomic carbon in the growth of hydrocarbon chains has been obtained by Biloen *et al.* (*11*). In these studies nickel, cobalt, and ruthenium catalysts were precovered with ^{13}C atoms produced by the disproportionation of ^{13}CO. The adsorbed ^{13}CO was exchanged with ^{12}CO and the catalysts were then exposed

0021-9517/81/080418-15$02.00/0

to a mixture of ^{12}CO and H_2. Careful mass spectrometric analysis of the products showed a random distribution of ^{12}C and ^{13}C among the hydrocarbons, consistent with the initial inventories of the two isotopes. It was also found that the time needed to convert ^{13}C atoms and ^{12}CO molecules to methane were nearly identical. From these observations it was concluded that CO dissociation is very rapid and hence is unlikely to be a rate-limiting step, that CH_x ($x = 0$–3) species constitute the most reactive C_1 surface species, and that methane and other hydrocarbons are formed from the same building blocks. These conclusions have also been supported by the analysis of methane synthesis kinetics reported by Ekerdt and Bell (*12*) and by the observation of a significant inverse H_2/D_2 isotope effect on methane synthesis recently reported by Kellner and Bell (*13*).

The proposition that hydrocarbon chain growth can occur on a ruthenium surface via a polymerization mechanism involving methylene groups as the monomer has recently been supported by the work of Brady and Petit (*14*). These authors demonstrated that a spectrum of hydrocarbons, resembling that obtained by CO hydrogenation, can be formed by reaction of CH_2N_2 and H_2 over ruthenium and other Groups VIII metals. The results were explained by suggesting that the decomposition of CH_2N_2 acts as a source of methylene groups, a part of which is converted to methyl groups by reaction with adsorbed hydrogen. It was proposed that the methyl groups then act as initiators for chain growth. The applicability of these results and their interpretation to hydrocarbon synthesis from CO and H_2 is supported by the work of Bell and co-workers (*15, 16*). Their work has shown that methyl, methylene, and higher-molecular-weight alkyls present on a ruthenium surface can be detected through the reaction of these species with olefins, and that the consumption of surface methylene groups by this means inhibits the propagation of hydrocarbon chain growth.

In the present study an investigation has been carried out of the kinetics of hydrocarbon synthesis over an alumina-supported ruthenium catalyst. Emphasis was placed on establishing the influence of reaction conditions on the rates of product formation, the distribution of olefins and paraffins according to carbon number, and the ratio of olefin to paraffin obtained for each carbon number. These data were then used to evaluate theoretical expressions for the reaction kinetics, derived from a comprehensive mechanism for hydrocarbon synthesis.

EXPERIMENTAL

A 1% Ru/Al_2O_3 catalyst was prepared by adsorption of $Ru_6C(CO)_{17}$ from pentane solution onto Kaiser KA-201 γ alumina. Details concerning synthesis of the complex and the impregnation procedure have been described previously (*17*). Once dried, the catalyst was reduced in flowing H_2. Reduction was begun slowly raising the temperature from 298 to 673 K and continued by maintaining it at 673 K for 8 hr. The dispersion of the freshly reduced catalyst was determined to be 1.0 by H_2 chemisorption.

A stainless-steel microreactor heated in a fluidized bed was used for all of the work reported here. Reactants were supplied from a high-pressure cylinder containing a desired ratio of H_2 and CO. The reaction products were analyzed by gas chromatography using flame ionization detection. A balanced pair of 2.4-mm × 1-m stainless-steel columns packed with Chromsorb 106 was used to separate C_1 through C_5 paraffins and olefins. A 0.25-mm × 35-m glass capillary column coated with OV-101 was used to separate C_5 through C_{10} paraffins and olefins. Complete product distributions were determined by normalizing the analyses for the C_5 products obtained from the packed and capillary columns.

Prior to each series of experiments, 100 mg of the (+120, −80 mesh) catalyst was reduced in flowing H_2 for 10 to 12 hr at 673

K and 10 atm. The temperature was then lowered to 498 K and the feed mixture was introduced at a flowrate of 200 cm^3/min (NTP). Ten minutes after the reaction had begun, a gas sample was taken for analysis and the gas feed was switched over to pure H_2 for 1 hr. This break-in period for a fresh catalyst charge was accompanied by a reduction in the Ru dispersion from 1.0 to 0.6. Once a stable activity had been obtained, the reaction conditions were adjusted to those desired for a particular experiment. Periodically, data were taken at 498K, 10 atm, and $H_2/CO = 3$ to determine whether changes in catalyst activity had occurred. In all cases, activities were reproduced to within a few percent. Maintaining the catalyst in H_2 for prolonged periods was also determined to have no effect on catalyst activity.

RESULTS

The primary hydrocarbon products produced under all reaction conditions were α-olefins and normal paraffins. Resolution between the olefinic and paraffinic products at each carbon number was excellent in most cases, but some loss in resolution did occur for products containing 7 to 10 carbon atoms when conditions favoring a very high olefin to paraffin ratio were used. Branched hydrocarbons and β-olefins were also detected but usually in much smaller concentrations than those of the primary products. The oxygen released in conjunction with the synthesis of hydrocarbons appeared as water and only negligible quantities of carbon dioxide were detected. The only other oxygenated product formed in significant quantities was methanol. The concentration of this product relative to the concentration of hydrocarbons was a strong function of reaction conditions. Thus, for example, the ratio of methanol to methane approached unity at low temperatures, and high pressures and H_2/CO ratios, but decreased to 0.17 as the temperature was increased and/or the pressure and H_2/CO ratio were decreased. Since the focus of the present study is on the synthesis of hydrocarbons, a discussion of methanol synthesis and its relation to the synthesis of hydrocarbons will be presented elsewhere (*18*).

The rate of methane formation was measured at pressures between 1 and 10 atm, temperatures between 448 and 548, and H_2/CO ratios of 1, 2, and 3. By using a feed flow rate of 200 cm^3/min (NTP), the conversion of CO could always be held well below 1.5%. The accumulated data were fitted, by means of a nonlinear least-squares regression, to the power law expression given by

$$N_{C_1} = 1.3 \times 10^9 \exp(-28{,}000/RT) P_{H_2}^{1.35}/P_{CO}^{0.99}.$$

In this equation, N_{C_1} is the turnover number for methane formation (based on a Ru dispersion of 0.6), and P_{H_2} and P_{CO} are the partial pressures of H_2 and CO, respectively, expressed in atmospheres. Figure 1 illustrates the quality of agreement between rates calculated using the above equation and those determined experimentally. The average deviation between experiment and correlation is less than $\pm 6\%$.

Seventy to eighty percent of the hydrocarbon products were analyzed to be C_2 through C_{10} paraffins and olefins. Examples of the ratio of the formation of hydrocar-

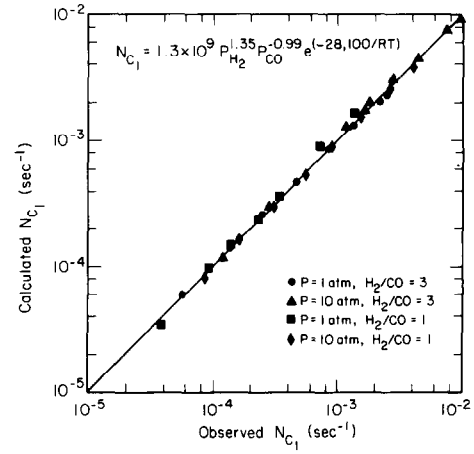

FIG. 1. Cross plot of predicted versus observed rates of methane synthesis.

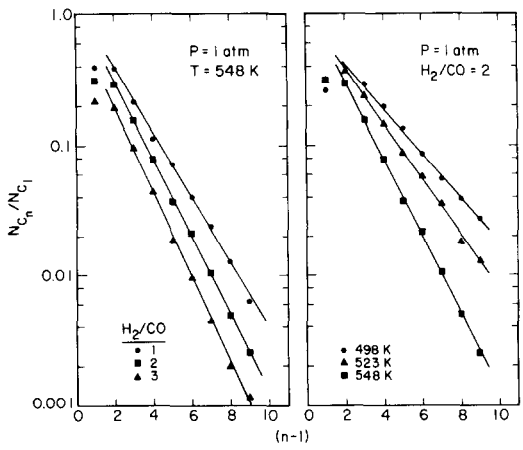

FIG. 2. Distribution of C_1 through C_{10} hydrocarbons observed at 1 atm: (a) effects of H_2/CO ratio; (b) effects of temperature.

bons containing n carbon atoms to the rate of methane formation are shown in Figs. 2 and 3. Figure 2 shows that with the exception of the points for $n = 2$ all of the data taken at 1 atm lie along straight lines on the coordinates of log (N_{C_n}/N_{C_1}) versus $(n - 1)$. The decreasing slope of the lines as either the H_2/CO ratio or the temperature is decreased is indicative of an increase in the average molcular weight of the products. The data taken at 10 atm (Fig. 3) also lie along straight lines on the indicated coordinates, but in this case deviations are seen for $n = 2$ and 3. When either the H_2/CO ratio or the temperature is decreased, the slope of the lines in Fig. 3 decrease slightly, and the lines appear to be translated upward in a near parallel fashion.

The kinetics for the synthesis of C_2 through C_{10} olefins and paraffins can also be represented by power law rate expressions. Parameter values obtained by fitting the data to such expression are presented in Tables 1 and 2. Examination of Table 1 shows that a positive order dependence on H_2 and a negative order dependence on CO partial pressures is observed in all cases. For a given carbon number, the H_2 dependence for paraffin formation is higher than that for olefin formation, whereas the CO dependence is more nearly the same for both products. The data in Table 1 also indicate that the magnitudes of m and n for the formation of olefins decrease substantially with increasing carbon number. While there is some indication of a similar trend for the paraffins, the pattern is not as clearly evident as for the olefins.

The information presented in Table 2 shows that the activation energy for olefin synthesis is higher than that for paraffin synthesis, suggesting that the olefin to paraffin ratio in the products should increase with increasing temperature. The

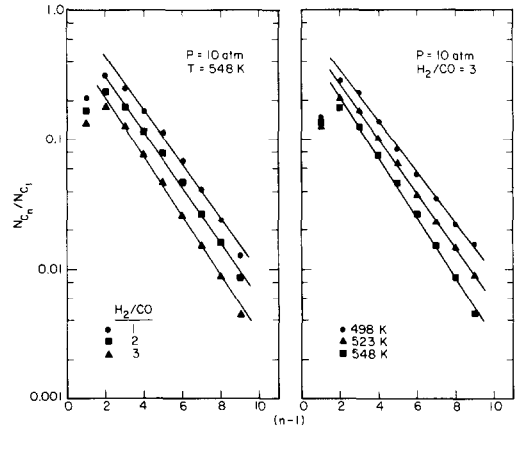

FIG. 3. Distribution of C_1 through C_{10} hydrocarbons observed at 10 atm: (a) effects of H_2/CO ratio; (b) effects of temperature.

TABLE 1

Dependencies of the Rates for the Synthesis of C_1 through C_{10} Hydrocarbons on the Partial Pressures of H_2 and CO[a]

	Olefin			Paraffin		
C_n	m	n	% Dev.[b]	m	n	% Dev.[b]
C_1	—	—	—	1.31	−0.96	7.7
C_2	0.82	−0.73	4.8	1.45	−0.85	7.7
C_3	0.80	−0.55	3.2	1.37	−0.49	4.9
C_4	0.74	−0.47	3.0	1.21	−0.46	3.3
C_5	0.53	−0.36	8.1	0.86	−0.24	2.3
C_6	0.47	−0.28	6.3	1.11	−0.32	13.5
C_7	0.35	−0.19	9.3	0.94	−0.24	5.9
C_8	0.31	−0.15	11.5	0.91	−0.27	7.9
C_9	0.20	−0.05	12.3	0.50	−0.18	19.4
C_{10}	0.17	−0.01	15.4	0.93	−0.35	11.4

[a] Reaction conditions: T = 498 K; P = 1–10 atm; H_2/CO = 1–3.
[b] Average deviation between predicted and observed rates.

TABLE 2

Power Law Rate Expressions[a] for the Synthesis of C_1 through C_4 Hydrocarbons[b]

C_n	A [atm$^{(m-n)}$ s^{-1}]	m	n	E_a (kcal/mole)	% Dev.[c]
C_1	1.3×10^9	1.35	−0.99	28	5.6
$C_2^=$	2.5×10^8	0.74	−0.68	28	5.7
C_2^-	1.6×10^6	1.34	−0.81	25	11.3
$C_3^=$	2.3×10^7	0.82	−0.58	25	4.2
C_3^-	1.4×10^3	1.39	−0.55	18	5.8
$C_4^=$	3.8×10^6	0.70	−0.44	24	9.6
C_4^-	8.7×10^3	1.14	−0.47	19	4.8

[a] $N_{C_n} = A \exp(-E_a/RT) P_{H_2}^m P_{CO}^n$.
[b] Reaction conditions: T = 448–548 K; P = 1–10 atm; H_2/CO = 1–3.
[c] Average deviation between predicted and observed rates.

extent to which this trend is observed is illustrated in Fig. 4. Below about 498 K, the plots of log $(N_{C_n^=}/N_{C_n^-})$ versus $1/T$ are linear for n = 2, 3, and 4. From the slope of this portion of the plots, the difference in activation energies for the formation of olefins and paraffins is estimated to be about 6 kcal/mole. The sharp decline in log $(N_{C_n^=}/N_{C_n^-})$ which occurs at temperatures above 498 K can be ascribed to hydrogenation of the olefins. This interpretation was confirmed by examining the effects of reactant space velocity on the olefin to paraffin ratio. At temperatures below 498 K, this ratio is independent of space velocity, but as the temperature is increased above 498 K, the ratio of olefins to paraffins decreases with decreasing space velocity.

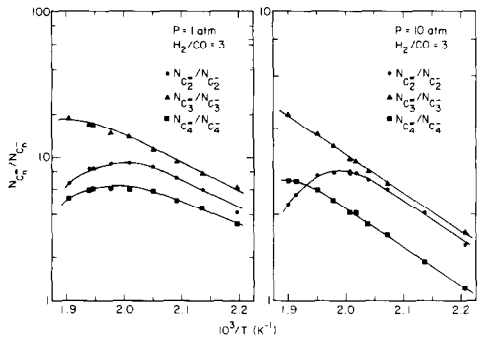

FIG. 4. Effects of temperature on the olefin to paraffin ratio of C_2 through C_4 products: (a) P = 1 atm; (b) P = 10 atm.

Since it has been reported that olefins formed via primary reactions can be incorporated to form higher-molecular-weight products (*7, 15*), an investigation was made to establish the possible influence of such reactions on the observed product distributions. When ethylene was added to the synthesis gas at levels similar to those produced by the reaction, no evidence could be observed for olefin incorporation. Raising the level of ethylene addition to 0.5 or 1.0% of the total feed (20 to 40 times that normally found in the reaction products) did produce an effect on the distribution of products, as can be seen in Fig. 5. The

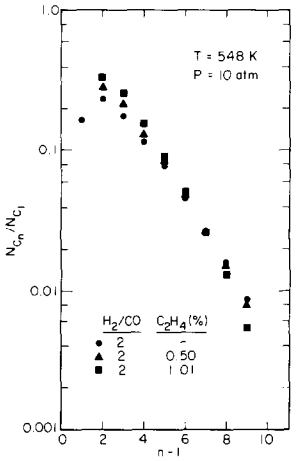

FIG. 5. Effects of ethylene addition on the distribution of C_1 through C_{10} hydrocarbons.

formation of C_3 and C_4 products is increased, but the formation of C_{6+} products is suppressed. The extent to which these changes occur increases with the level of ethylene addition. A similar trend was also observed for data taken at 1 atm and 498 K.

DISCUSSION

The kinetics of hydrocarbon synthesis presented here can be interpreted in terms of the mechanism shown in Fig. 6. Detailed discussions of the experimental evidence supporting this view of CO hydrogenation have recently been presented in a number of reviews (*1–7*). Consequently, the justification for including particular steps, and for assuming that certain of these are reversible, will be restricted to ruthenium.

It is proposed that CO is first adsorbed into a molecular state from which dissociative adsorption can then occur. Infrared studies reported by a number of authors (*12, 19–21*) indicate that the surface of Ru is nearly saturated by molecularly adsorbed CO under reaction conditions. The reversibility of molecular adsorption is supported by recent isotopic substitution studies performed with ^{12}CO and ^{13}CO which indicate that equilibration of the surface with the gas phase is very rapid under reaction conditions (*22*). Low and Bell (*10*) have shown that CO disproportionation will occur to a significant degree over Ru/Al_2O_3 for temperatures in excess of 423 K. These results suggest that CO dissociation is an activated process. More recently, TPD experiments performed by McCarty and Wise (*23*) have demonstrated that the recombination of carbon and oxygen atoms and the desorption of CO are very rapid since extensive scrambling of preadsorbed $^{13}C^{16}O$ and $^{12}C^{18}O$ was observed at temperatures above 473 K, where hydrocarbon synthesis normally occurs.

The adsorption of H_2 is assumed to occur dissociatively, and to be reversible. This view is supported by H_2/D_2 scrambling studies performed in the presence of CO over a Ru/SiO_2 catalyst (*22*). The results of these experiments show that above 423 K, the extent of scrambling is very close to that predicted at equilibrium, indicating that the rates of $H_2(D_2)$ adsorption, reaction, and desorption are faster than the rate of hydrocarbon synthesis.

It is well recognized that during CO hydrogenation over Ru, water is the primary product via which oxygen is removed from the catalyst surface (*12*). The mechanism of forming water in the presence of substantial amounts of adsorbed CO is not known and may occur via either a sequence of Langmuir–Hinshelwood steps or a concerted Rideal–Eley step. For the purposes of the present discussion it has been assumed that the latter process represents the dominant reaction path.

The stepwise hydrogenation of single carbon atoms is taken as the starting point for hydrocarbon synthesis. Studies by a number of investigators (*9–11*) have shown that atomic carbon produced by either CO disproportionation or CO hydrogenation is extremely reactive and will form methane and higher-molecular-weight hydrocarbons upon hydrogenation. Furthermore, the work of Biloen *et al.* (*11*) has demonstrated that the incorporation of carbon into hydrocarbons occurs with equivalent ease from molecularly adsorbed CO and atomically adsorbed C, indicating that the dissociation of adsorbed CO is not a rate-limiting step in the formation of hydrocarbons. This conclusion is supported further by the recent

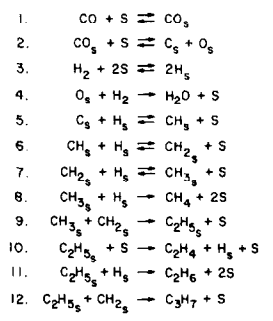

FIG. 6. Proposed mechanism of hydrocarbon synthesis from CO and H_2.

studies of Kellner and Bell (*13*) in which evidence was reported for a strong inverse H_2/D_2 isotope effect on the synthesis of methane over two Ru/Al_2O_3 catalysts and a similar, albeit weaker effect for synthesis over a Ru/SiO_2 catalyst. The authors noted that the more rapid formation of CD_4 than CH_4 indicates that one or more of the elementary steps preceeding the rate-limiting step involves the addition of hydrogen and is at equilibrium (e.g., steps 5 through 7).

The methyl groups produced in step 7 are precursors to the formation of methane and the growth of hydrocarbon chains. The former process occurs by the addition of a hydrogen atom to the methyl group and the latter by the insertion of a methylene group into the metal–carbon bond of the methyl group. Once started, chain growth can continue by further addition of methylene units to the alkyl intermediates. Termination of chain growth is postulated to occur via one of two processes—hydrogen addition to form normal alkanes and β-elimination of hydrogen to form α-olefins. Thus, one may visualize the formation of C_{2+} hydrocarbons as a polymerization process in which methylene groups act as the monomer and the alkyl groups are the active centers for chain growth.

The proposed mechanism of methanation and chain growth is strongly supported by the results of several recent studies. Brady and Petit (*14*) have demonstrated that hydrocarbons can be formed by the decomposition of diazomethane over supported Ru, as well as other Group VIII metals. In the absence of H_2, ethylene is the only product observed. When H_2 is added to the flow of CH_2N_2, a product distribution resembling that observed during CO hydrogenation is obtained. The authors propose that methylene groups produced by the decomposition of CH_2N_2 react in the absence of adsorbed hydrogen to form ethylene. In the presence of adsorbed hydrogen, methyl groups are formed. The addition of methylene units to these species initiates chain growth. Direct evidence for the presence of methylene and C_1 through C_4 alkyl groups on the surface of Ru have recently been obtained using the technique of reactive scavenging (*15, 16*). In these studies a small amount of cyclohexene is added to the synthesis gas. The products are observed to contain norcarane; methylcyclohexene; and methyl-, ethyl-, propyl-, and butylcyclohexane in addition to the usual spectrum of hydrocarbons obtained by CO hydrogenation. The appearance of products derived from cyclohexene is explained by the reaction of cyclohexene with methylene and alkyl groups, formed on the catalyst surface from CO and H_2.

Rate expressions describing the kinetics of forming methane and higher-molecular-weight hydrocarbons can be derived on the basis of the mechanism shown in Fig. 6, following the introduction of a number of simplifying assumptions. To begin with, it is assumed that the rate of methane formation is controlled by step 8 and that the steps preceeding it are at equilibrium. This assumption is supported by the observation of a significant inverse H_2/D_2 isotope effect on the rate of methane formation over a Ru/Al_2O_3 catalyst identical to that used in the present studies (*13*). Next, it is assumed that steps 9, 10, and 11 are irreversible and that the rate coefficients for these steps are independent of the chain length, n. The validity of this assumption will be discussed following the derivation of rate expressions for C_{2+} hydrocarbons. Finally, it will be assumed that the fraction of vacant surface sites can be expressed as

$$\theta_v = 1/K_1 P_{CO}, \qquad (1)$$

where K_1 is the equilibrium constant for reaction 1. Equation (1) is based on the infrared observations reported by Kellner and Bell (*21*) which show that under reaction conditions the Ru surface sites active in hydrocarbon synthesis are virtually saturated by linearly adsorbed CO and that the surface coverage by this species can be

represented by a Langmuir isotherm which only involves the partial pressure of CO.

The turnover number for methane formation, N_{C_1}, can be written as

$$N_{C_1} = k_8\theta_{CH_3}\theta_H, \quad (2)$$

where k_8 is the rate coefficient for step 8 in Fig. 6, θ_{CH_3} is the fractional coverage of the Ru surface by CH_3 groups, and θ_H is the fractional coverage by H atoms. Since equilibrium has been assumed for steps 1 through 3 and 5 through 7, θ_{CH_3} can be expressed as

$$\theta_{CH_3} = K_2K_3^{1.5}K_5K_6K_7P_{H_2}^{1.5}\theta_v/\theta_O, \quad (3)$$

where K_i is the equilibrium constant for the ith reaction and θ_O is the fractional coverage of the Ru surface by O atoms. The magnitude of θ_H is given by

$$\theta_H = K_3^{1/2}P_{H_2}^{1/2}\theta_v. \quad (4)$$

Substitution of Eqs. (3) and (4) into Eq. (2) and introduction of Eq. (1) for θ_v results in

$$N_{C_1} = k_8\frac{K_2K_3^2K_5K_6K_7}{K_1^2\theta_O}\frac{P_{H_2}^2}{P_{CO}^2}. \quad (5)$$

The dependence of N_{C_1} on θ_O can be eliminated from Eq. (5) if it is assumed that all of the carbon and oxygen released in step 2, which does not recombine to form adsorbed CO, reacts to form hydrocarbons and water. This implies that

$$N_{H_2O} = \sum_{n=1}^{\infty} nN_{C_n}, \quad (6)$$

where

$$N_{H_2O} = k_4\theta_O P_{H_2}. \quad (7)$$

Since all hydrocarbon products containing two or more carbon atoms must be formed by chain growth, step 9, the overall rate of carbon consumption for the formation of hydrocarbon products can be expressed as

$$\sum_{n=1}^{\infty} nN_{C_n} = k_8\theta_{CH_3}\theta_H + \sum_{n=1}^{\infty} k_p\theta_{CH_2}\theta_n, \quad (8)$$

where k_p is the rate constant for chain growth, step 9; θ_{CH_2} is the fractional coverage of the Ru surface by methylene groups; and θ_n is the fractional coverage of the Ru surface by alkyl groups of chain length n. Combining Eqs. (6)–(8) results in Eq. (9).

$$k_4\theta_O P_{H_2} = k_8\theta_{CH_3}\theta_H + \sum_{n=1}^{\infty} k_p\theta_{CH_2}\theta_n. \quad (9)$$

Equation 9 can be solved for θ_O in the limits where either methane or higher molecular weight products predominate. For the first case $N_{C_1} \gg \sum_{n=2}^{\infty} nN_{C_n}$. Substitution of the expressions for θ_{CH_3} and θ_H into Eq. (9) results in

$$\theta_O = \frac{k_3}{K_1}\left(\frac{k_8}{k_4}K_2K_5K_6K_7\right)^{1/2}\frac{P_{H_2}^{1/2}}{P_{CO}}, \quad (10)$$

which, on substitution into Eq. (5), gives

$$N_{C_1} = k_e\frac{P_{H_2}^{1.5}}{P_{CO}}, \quad (11)$$

where

$$k_e = \frac{K_3}{K_1}(k_8k_4K_2K_5K_6K_7)^{1/2}. \quad (12)$$

This result is identical to that obtained by Ekerdt and Bell (*12*).

For the second case, it is assumed that $N_{C_1} \ll \sum_{n=2}^{\infty} nN_{C_n}$ so that the first term on the right-hand side of Eq. (9) can be neglected. To solve for θ_O in this case requires the development of expressions for θ_{CH_2} and θ_n. An expression for θ_{CH_2} can be derived from the equilibrium relationships existing between steps 1, 2, 3, 5, and 6. Thus

$$\theta_{CH_2} = \frac{K_2K_3K_5K_6}{K_1\theta_O}\frac{P_{H_2}}{P_{CO}}. \quad (13)$$

An expression for θ_n can be obtained by imposing a steady-state balance on the formation of alkyl groups containing n carbon atoms.

$$0 = k_p\theta_{n-1}\theta_{CH_2} - k_p\theta_n\theta_{CH_2} - k_{tp}\theta_n\theta_H - k_{to}\theta_n\theta_v, \quad (14)$$

where k_{to} and k_{tp} are the rate coefficients for the formation of olefins and paraffins, steps

10 and 11 in Fig. 6. Solving for θ_n results in

$$\theta_n = \frac{k_p\theta_{CH_2}\theta_{n-1}}{k_p\theta_{CH_2} + k_{tp}\theta_H + k_{to}\theta_v}. \quad (15)$$

Equation (15) can be rewritten in terms of the probability of chain propagation, α, as

$$\theta_n = \alpha^{n-1}\theta_{CH_3}. \quad (16)$$

Comparing Eqs. (15) and (16) shows that

$$\alpha = \frac{k_p\theta_{CH_2}}{k_p\theta_{CH_2} + k_{to}\theta_v + k_{tp}\theta_H}. \quad (17)$$

The sum $\sum_{n=1}^{\infty} \theta_n$, appearing in Eq. (9), can now be expressed in closed form as

$$\sum_{n=1}^{\infty} \theta_n = \frac{\theta_1}{(1-\alpha)}. \quad (18)$$

If α is taken to be independent of P_{H_2} and P_{CO}, an assumption which is not rigorously correct but does not lead to significant error, then an expression for θ_O can be obtained by substitution of Eqs. 13 and 18 into Eq. 9. Thus,

$$\theta_O = \left[\frac{k_p K_2^2 K_3^{2.5} K_5^2 K_6^2 K_7}{k_4 K_1^2(1-\alpha)}\right]^{0.33} \frac{P_{H_2}^{0.5}}{P_{CO}^{0.67}} \quad (19)$$

Finally, substitution of Eq. (19) into Eq. (5) results in

$$N_{C_1} = k_e P_{H_2}^{1.5}/P_{CO}^{1.33}, \quad (20)$$

where

$$k_e = k_8\left[\frac{k_4 K_2 K_3^{2.5} K_5 K_6 K_7^2(1-\alpha)}{k_p K_1^4}\right]^{0.33}. \quad (21)$$

Table 3 presents a comparison between the predicted dependencies of N_{C_1} on the partial pressures of H_2 and CO and the dependencies determined from experimental data. It is apparent that the H_2 dependence contained in both limiting forms of the expression derived for N_{C_1} is in excellent agreement with that observed in this study, as well as others. The first of the two limiting forms for N_{C_1} also provides an accurate description of the CO dependence determined from the data taken in this study. It should be noted however that while Dalla Betta and Shelef (*24*) have also noted an inverse first order CO dependence, other investigators (*12, 25*) have found that the inverse dependence is less than first order.

Table 3 also presents a comparison between the apparent activation energies and preexponential factors for methane formation determined from the present results and those reported by previous investigators. It is seen that the activation energy determined in this study is about 4 kcal/mole higher than that reported earlier. At present there is no explanation for this difference. A substantial variation is observed in the values of the preexponential factors reported by different authors. It is conceivable that a major part of these differences may be related to the precision used in measuring the Ru dispersion and to the effects of dispersion on catalyst activity. As noted by King (*26*), and Kellner and Bell (*27*), the specific activity of Ru decreases as the dispersion of the metal increases.

Expressions describing the rates of formation of higher-molecular-weight products can be derived in a manner similar to that followed in developing an expression for the rate of methane formation. The turnover frequencies for the formation of normal paraffins and α-olefins can be expressed as follows:

$$N_{C_{\bar{n}}} = k_{tp}\theta_H\theta_n; \quad (22)$$

$$N_{C_{\bar{\bar{n}}}} = k_{to}\theta_v\theta_n. \quad (23)$$

Summing Eqs. (22) and (23) to obtain an expression for the rate of formation of products containing n carbon atoms and substituting from Eq. (16) for θ_n results in

$$N_{C_n} = (k_{to}\theta_v + k_{tp}\theta_H)\alpha^{n-1}\theta_{CH_3}. \quad (24)$$

Substitution of θ_{CH_3} by $N_{C_1}/(k_8\theta_H)$ and substitution from Eqs. (1) and (4) for θ_v and θ_H leads to

$$N_{C_n} = (1 + \beta/P_{H_2}^{0.5})\alpha^{n-1}N_{C_1}, \quad (25)$$

TABLE 3

Comparison of the Rate Expressions for Methane Synthesis Obtained from Experimental Data with Those Obtained Theoretically

	Theory		Experiment			
	Eq. (11)	Eq. (20)	This study	Dalla Betta *et al.* (*23*)	Vannice (*24*)	Ekerdt and Bell (*12*)
Catalyst	—	—	1% Ru/Al_2O_3	1.5% Ru/Al_2O_3	5% Ru/Al_2O_3	5% Ru/SiO_2
$A[atm^{(m-n)}\ s^{-1}]$	—	—	1.3×10^9	3.2×10^7	5.6×10^8	2.2×10^9
E_a(kcal/mole)	—	—	28.2	24	24.2	24.1
m	1.5	1.5	1.35	1.8	1.6	1.5
n	−1.0	−1.33	−0.99	−1.1	−0.6	−0.6

assuming that $k_{tp} = k_8$. The parameter β appearing in Eq. 25 is defined as

$$\beta = k_{to}/k_{tp}K_3^{1/2} \tag{26}$$

and is related to the ratio of olefin to paraffin formation in the following fashion:

$$N_{C_n^=}/N_{C_n^-} = \beta/P_{H_2}^{0.5}. \tag{27}$$

The form of Eq. (25) suggests that a plot of log (N_{C_n}/N_{C_1}) versus $(n - 1)$ should be a straight line with a slope given by log α. The results presented in Figs. 2 and 3 were plotted in this fashion. As was noted earlier, with the exception of the point for $n = 2$, the data taken at 1 atm are in good agreement with Eq. (25). At 10 atm, Eq. (25) also provides a good description of the data, with the exception of the points at $n = 2$ and 3. A more complete discussion of the slope of the lines shown in Figs. 2 and 3, and its dependence on reaction conditions, will be presented below.

It is of interest at this point to consider whether the kinetics represented by Eq. (25) are consistent with the type of product distribution described by Friedel and Anderson (*28*) and Henrici-Olivé and Olivé (*29*). According to these authors the fraction of the total carbon converted to hydrocarbons which contain n carbon atoms, f_n, should be given by

$$f_n = n\alpha^{n-1}(1 - \alpha)^2 \tag{28}$$

and, consequently, a plot of log (f_n/n) versus n should be a straight line of slope α and intercept log $[(1 - \alpha)^2/\alpha]$. The derivation of Eq. (28), which is often referred to as a Storch–Anderson or Schultz–Flory distribution in the recent literature on Fischer–Tropsch synthesis (*29–35*), is based on the assumption that chain growth occurs by the addition of single-carbon intermediates and that chain termination leads to the formation of stable products. No regard need be given in this derivation to the details of the chain propagation or termination steps.

The expressions contained in Eq. (25) for the kinetics of olefin and paraffin synthesis are consistent with a Storch–Anderson/Schultz–Flory distribution, provided one considers products of a homologous series, viz., only olefins or paraffins. This statement can be verified by starting out with the defining equations for the fraction of products within a homologous series, which contain a given number of carbon atoms:

$$f_n^- = nN_{C_n^-} \Big/ \sum_{n=1}^{\infty} nN_{C_n^-}, \tag{29}$$

$$f_n^= = nN_{C_n^=} \Big/ \sum_{n=2}^{\infty} nN_{C_n^=}. \tag{30}$$

Note that the summation for paraffins runs from one to infinity while that for olefins runs from two to infinity. Substitution of the first and second terms of Eq. (25) into

Eqs. (29) and (30), respectively, gives

$$f_n^- = n\alpha^{(n-1)}(1-\alpha)^2; \qquad (31)$$

$$f_n^= = \frac{n\alpha^{(n-1)}(1-\alpha)^2}{1-(1-\alpha)^2}. \qquad (32)$$

Equation (31) and the numerator of Eq. (32) are identical to Eq. (28). The denominator appearing in Eq. (32) arises from the fact that the summation of Eq. (30) begins with $n = 2$.

Figures 7 and 8 illustrate plots of $f_n^=/n$ and f_n^-/n versus $(n-1)$ for data obtained at 1 and 10 atm. Both figures show that, with the exception of the point at $n = 2$, the experimental values of $f_n^=/n$ fall along a straight line. The slope of the line is equal to log α, and, as can be seen in Table 4, the values of α determined from Figs. 7 and 8 are very close to those determined from plots of N_{C_n}/N_{C_1}. Equation (32) can be tested further by comparing the intercept of the line passed through experimental values of $f_n^=/n$ with the expression $(1-\alpha)^2/[1-(1-\alpha)^2]$ obtained from Eq. (32) for $(n-1) = 0$. Table 4 indicates that the intercepts evaluated from Figs. 7 and 8 are somewhat larger than those predicted by Eq. (32). This difference can be explained if it is assumed that the low value of $f_2^=/2$ is due to a partial conversion of ethylene to ethane. Under this circumstance the difference between $2\alpha(1-\alpha)^2/[1-(1-\alpha)^2]$ and the experimentally observed value of $f_2^=$ would correspond to the carbon number fraction of the ethylene converted to ethane. Imposing this correction leads to predicted intercepts which are in much closer agreement with those deduced from the experimental results.

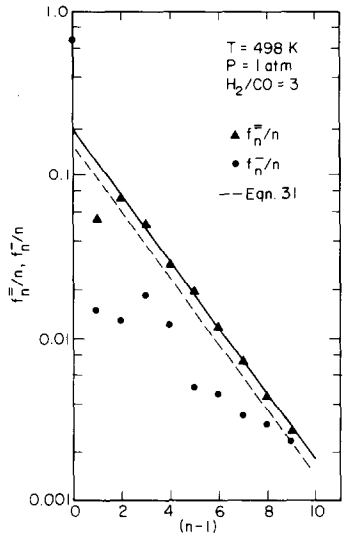

FIG. 7. Plots of $f_n^=/n$ and f^-/n versus $(n-1)$ for P = 1 atm: solid line, best fit through olefin data; dashed line, Eq. (31).

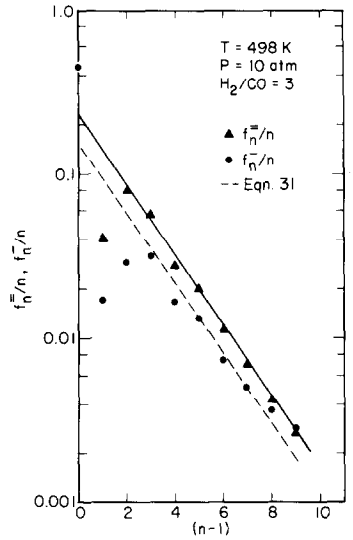

FIG. 8. Plots of $f_n^=/n$ and f_n^-/n versus $(n-1)$ for P = 10 atm: solid line, best fit through olefin data; dashed line Eq. (31).

Equation (31) predicts that the values of f_n^-/n should also lie along a straight line on a plot of log (f_n^-/n) versus $(n-1)$. The dashed line in Fig. 7 shows that at 1 atm the point for methane lines well above the line given by Eq. (31), the points for $n = 2$ through 8 fall below the line, and only the points for $n = 9$ and 10 lie near the line. The agreement between theory and experiment is somewhat better at 10 atm. In this case Fig. 8 shows that the point for methane lies above the line, the points for $n = 2$ and 3 lie below the line, but the points for $n = 4$ through 8 lie along the line. The remaining two points, for $n = 9$ and 10, lie slightly above the line. The pattern of the deviations between theory and experiment ob-

TABLE 4

Comparison of the Observed Product Distributions with Theoretically Predicted Distributions for Olefins and Paraffins

	P = 1 atm[a]		P = 10 atm[a]	
	Source	Value	Source	Value
α	Fig. 7	0.62	Fig. 8	0.61
α	Fig. 2	0.66	Fig. 3	0.63
$f_1^{=}$[b]	Fig. 7	0.20	Fig. 8	0.23
$f_1^{=}$	$\frac{(1-\alpha)^2}{[1-(1-\alpha)^2]}$	0.18	$\frac{(1-\alpha)^2}{[1-(1-\alpha)^2]}$	0.17
$f_1^{=}$	—[c]	0.20	—[c]	0.20
f_1^{-}	Fig. 7	0.66	Fig. 8	0.44
f_1^{-}	$(1-\alpha)^2$	0.14	$(1-\alpha)^2$	0.15
f_1^{-}	—[d]	0.64	—[d]	0.41

[a] T = 498 K; H_2/CO = 3.

[b] Intercept at $(n-1)=0$.

[c] $f_1^{=} = (1-\alpha)^2/[1-(1-\alpha)^2]/\{1-2\{\alpha(1-\alpha)^2/[1-(1-\alpha)^2]-f_2^{=}/2\}\}$.

[d] $f_1^{-} = (1-\alpha)^2 + \sum_{n=2}^{\infty} n[\alpha^{(n-1)}(1-\alpha)^2 - f_n^{-}/n]$.

served in Figs. 7 and 8 suggests that a part of the C_{2+} paraffinic product undergoes hydrogenolysis to form methane. Based on this interpretation, the correct value of f_1^- should be given by

$$f_1^- = (1-\alpha)^2 + \sum_{n=2}^{\infty} n[\alpha^{(n-1)}(1-\alpha)^2 - f_n^-/n]. \quad (33)$$

Values of f_1^- determined in this fashion are listed in Table 4 and are seen to be in good agreement with the values of f_1^- observed experimentally. The fact that the formation of excess methane is lower at higher pressure is consistent with the proposed interpretation. For the same H_2/CO ratio, elevation of the total pressure causes a reduction in θ_v, due to the higher CO partial pressure, and, hence, a reduction in the availability of sites for paraffin adsorption. The decline in the extent of paraffin hydrogenolysis with increasing carbon number might be ascribed to the fact that with increasing molecular weight a higher number of contiguous vacant sites might be required for initial adsorption. Finally, it should be noted that in addition to explaining the discrepancies in the distribution of paraffins presented in Figs. 7 and 8, the occurrence of hydrogenolysis would explain why in Figs. 2 and 3 the experimental points for n = 2 and 3 fall below a straight line passed through the balance of the data, and why extrapolation of the lines in these figures to $(n-1)=0$ leads to an intercept of less than unity.

The form of Eq. (27) indicates that plots of $N_{C_n^=}/N_{C_n^-}$ versus $P_{H_2}^{-0.5}$ should result in straight lines with a slope of β which is independent of n. Figure 9 illustrates a test of this prediction for n = 2, 3, and 4. The data plotted in this figure were taken at pressures between 1 and 10 atm and H_2/CO ratios between 1 and 3, and at a temperature of 498 K to minimize the effects of olefin hydrogenation. For each value of n the data are seen to scatter around a straight line, in general agreement with Eq. (27) and consistent with the empirical rate expressions presented in Table 1. It is apparent, though, that the slopes of the lines are dependent on the value of n. This dependence is seen even more clearly in Fig. 10 which shows a plot of β versus n for n = 2 through 10. In the light of the discussion presented in connection with Figs. 7 and 8, it seems reasonable to propose that the high values of β for n = 2 and

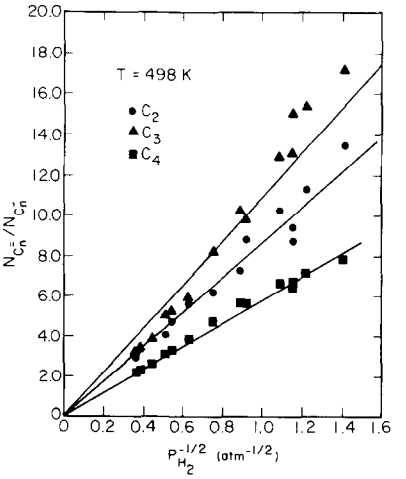

FIG. 9. Plots of $N_{C_n^=}/N_{C_n^-}$ versus $P_{H_2}^{-0.5}$.

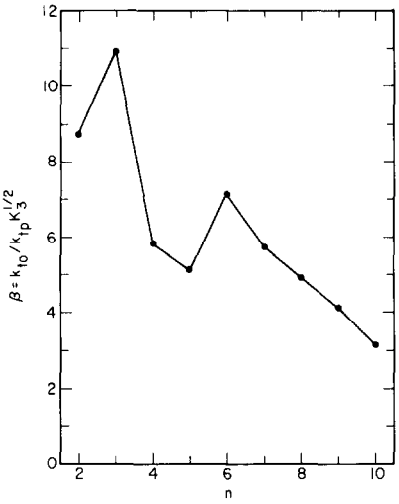

FIG. 10. Plot of β versus n.

3 may be due, in part, to a partial hydrogenolysis of ethane and propane. The balance of the variation in β with n may be due to a dependence of the rate coefficients for chain termination on the value of n. A more detailed interpretation of these observations is not possible at present and must await further study.

The temperature dependence of $N_{C_n^=}/N_{C_n^-}$, which was shown in Fig. 4, can be interpreted in terms of the rate and equilibrium constants appearing in the definition of β, Eq. (26). The difference in the apparent activation energies for the formation of olefins and paraffins, E_{op}, are related to the activation energies for the reactions of allyl species to form olefins and paraffins, E_o and E_p, and to the heat of H_2 adsorption, ΔH_{H_2}, by the following expression

$$E_{op} = E_o - E_p - \Delta H_{H_2}/2. \quad (34)$$

Assuming that ΔH_{H_2} is about -20 kcal/mole, a value typical for group VIII metals (*36*), leads to the conclusion that $(E_p - E_o) \simeq 4$ kcal/mole.

A relationship for the dependence of α, the probability of chain growth, on the partial pressures of H_2 and CO can be determined starting from the definition for α, Eq. (17). Substitution of Eqs. (1), (4), (13), and (19) for θ_v, θ_H, θ_{CH_2}, and θ_O (assuming that $N_{C_1} \ll \sum_{n=2}^{\infty} nN_{C_n}$) gives the following expression:

$$\alpha = [1 + \gamma(1 - \alpha)^{-0.33}P_{CO}^{-0.67}(1 + \beta P_{H_2}^{0.5})]^{-1}, \quad (35)$$

where

$$\gamma = \left[\frac{K_3}{k_p^2 k_4 K_1^2 K_2 K_5 K_6}\right]^{0.33} \quad (36)$$

Rearrangement of Eq. (35) provides a more explicit equation for α, which can be solved by means of trial and error.

$$\alpha^{-1}(1 - \alpha)^{1.33} = \gamma P_{CO}^{-0.67}(1 + \beta P_{H_2}^{-0.5}) \quad (37)$$

The utility of Eq. (37) as a representation for the dependence of α on the partial pressures of H_2 and CO, and on the temperature can now be examined. To do so requires that values of β and γ be determined first. An expression for β can be obtained from the data presented in Figs. 4 and 10. Choosing the value of β for $n = 4$ as being representative leads to the following equation:

$$\beta = 1.8 \times 10^3 \exp(-5700/RT). \quad (38)$$

An equation for γ can be obtained by forcing an agreement between Eq. (37) and the values of α determined at 1 atm for $H_2/CO = 2$ and temperatures of 498, 523, and 548 K. The resulting expression is given by

$$\gamma = 1.2 \exp(-4{,}100/RT). \quad (39)$$

A comparison between the experimental and predicted values of α is presented in Table 5. It is observed that at 1 atm, Eq. (37) provides an accurate representation of the dependence of α on temperature as well as H_2 and CO partial pressures. When the total pressure is increased to 10 atm Eq. (37) predicts values of α which are substantially higher than those observed experimentally. Nevertheless, the reduced dependence of α on H_2 and CO partial pressures observed at 10 atm is properly reflected.

The failure of Eq. (37) to provide an

TABLE 5

Comparison of Predicted and Experimentally Observed Values of α

P (atm)	T (K)	H_2/CO	α	
			Predicted	Experimental
1	548	1	0.55	0.56
		2	0.52	0.51
		3	0.49	0.47
1	523	1	0.63	0.62
		2	0.60	0.61
		3	0.57	0.60
1	498	1	0.71	0.69
		2	0.68	0.68
		3	0.66	0.66
10	548	1	0.90	0.61
		2	0.89	0.60
		3	0.88	0.58
10	523	3	0.91	0.61
10	498	1	0.94	0.67
		2	0.94	0.63
		3	0.93	0.63

accurate estimation of α at 10 atm is not well understood. A possible explanation might be that at higher pressures additional termination steps become important. Inspection of Eq. (17) shows that this would cause a decrease in α. A reaction which might contribute to such an effect would be the insertion of CO into the metal–carbon bond of an alkyl group to form an acyl species which might subsequently react to produce either an aldehyde or an alcohol. Alternatively, one might consider the reaction of surface methylene or alkyl groups with olefins present in the reaction products (*15, 16*). The results presented in Fig. 5 show that under the reaction conditions used in the present work, ethylene does not participate extensively in this type of reaction. However, this does not exclude the possibility that higher-molecular-weight olefins might be more reactive than ethylene. As a consequence further investigation will be needed to establish the effects of additional chain termination reactions and secondary reactions on the magnitude of α.

CONCLUSIONS

In the present paper it has been shown that the reaction mechanism presented in Fig. 6 explains many aspects of CO hydrogenation over Ru. Rate expressions derived from this mechanism accurately describe the kinetics for the synthesis of methane and higher molecular weight hydrocarbons. It has been shown that C_{2+} olefins and paraffins are formed from a common precursor, and that, in the absence of further olefin hydrogenation, the olefin to paraffin ratio in the products depends only on the H_2 partial pressure. It has also been demonstrated that the products in a homologous series follow a Storch–Anderson/Schultz–Flory distribution. Minor deviations from such a distribution observed for olefins can be ascribed to a partial conversion of ethylene to ethane. The much more significant deviations found for paraffins appears to be due to a partial hydrogenolysis of C_{2+} alkanes, a process which seems to predominate at low CO partial pressures. Finally, it is concluded that the proposed mechanism can be used to deduce an expression for the effects of reaction conditions on the probability of chain growth, α. This expression provides an excellent correlation of the experimental results obtained at 1 atm but overpredicts the values of α observed at 10 atm. It is hypothesized that the discrepancy observed at higher pressures may indicate the presence of chain termination processes not included in the proposed mechanism.

ACKNOWLEDGMENT

The authors wish to express their appreciation to Professor Earl Muetterties for the helpful discussions of the reaction mechanism proposed here. This work was supported by the Division of Chemical Sciences, Office of Basic Energy Sciences, U.S. Department of Energy under Contract W-7405-ENG-48.

REFERENCES

1. Vannice, M. A., *Catal. Rev. Sci. Eng.* **14**, 153 (1976).
2. Ponec, V., *Catal. Rev. Sci. Eng.* **18**, 151 (1978).
3. Ponec, V., and von Barneveld, W. A., *I&EC Prod. Res. Develop.* **18**, 268 (1979).

4. Muetterties, E. L., and Stein, J., *Chem. Rev.* **80**, 479 (1979).
5. Biloen, P., *J. Roy. Neth. Chem. Soc.* **99**, 33 (1980).
6. Biloen, P., and Sachtler, W. M. H., *in* "Advances in Catalysis." Academic Press, New York, in press.
7. Bell, A. T., *Catal. Rev. Sci. Eng.* **23**, 203 (1981).
8. Singh, K. J., and Grenga, H. E., *J. Catal.* **47**, 328 (1977).
9. Rabo, J. A., Risch, A. P., and Poutsma, M. L., *J. Catal.* **53**, 295 (1978).
10. Low, G., and Bell, A. T., *J. Catal.* **57**, 397 (1979).
11. Biloen, P., Helle, J. N., and Sachtler, W. M. H., *J. Catal.* **58**, 95 (1979).
12. Ekerdt, J. G., and Bell, A. T., *J. Catal.* **58**, 170 (1979).
13. Kellner, C. S., and Bell, A. T., *J. Catal.* **67**, 175 (1981).
14. Brady, G. III, and Pettit, R., *J. Amer. Chem. Soc.* **102**, 6181 (1980).
15. Ekerdt, J. G., and Bell, A. T., *J. Catal.* **62**, 19 (1980).
16. Baker, J., and Bell, A. T., M.S. thesis, Department of Chemical Engineering, University of California, Berkeley, 1981.
17. Kuznetsov, V. L., Bell, A. T., and Yermakov, Yu. I., *J. Catal.* **65**, 374 (1980).
18. Kellner, C. S., and Bell, A. T., *J. Catal.* **71**, in press.
19. Dalla Betta, R. A., and Shelef, M., *J. Catal.* **48**, 111 (1977).
20. King, D. L., *J. Catal.* **61**, 77 (1980).
21. Kellner, C. S., and Bell, A. T., *J. Catal.* **71**, in press.
22. Cant, N., and Bell, A. T., unpublished results.
23. McCarty, J. G., and Wise, H., *J. Catal.* **60**, 204 (1979).
24. Dalla Betta, R. A., Piken, A. G., and Shelef, M., *J. Catal.* **35**, 53 (1974).
25. Vannice, M. A., *J. Catal.* **37**, 449, 462 (1975).
26. King, D. L., *J. Catal.* **51**, 386 (1978).
27. Kellner, C. S., and Bell, A. T., submitted for publication.
28. Friedel, R. A., and Anderson, R. B., *J. Amer. Chem. Soc.* **72**, 1212, 2307 (1950).
29. Henrici-Olivé, G., and Olivé, S. *Angew. Chem. Int. Engl. Ed.* **15**, 136 (1976).
30. Dautzenberg, I. M., Helle, J. N., von Santen, R. A., and Verbeck, H., *J. Catal.* **50**, 8 (1977).
31. Anderson, R. B., *J. Catal.* **55**, 114 (1978).
32. Madon, R. J., *J. Catal.* **57**, 183 (1979).
33. Henrici-Olivé, G., and Olivé, S., *J. Catal.* **60**, 481 (1979).
34. Anderson, R. B., *J. Catal.* **60**, 484 (1979).
35. Madon, R. J., *J. Catal.* **60**, 485 (1979).
36. Toyoshima, I., and Somoriai, G. A., *Catal. Rev. Sci. Eng.* **19**, 105 (1979).